Monosynaptic convergence of somatic and visceral C-fiber afferents on projection and local circuit neurons in lamina I: a substrate for referred pain

Liliana L. Luz[a,b,c], Elisabete C. Fernandes[a,b], Miklos Sivado[d,e], Eva Kokai[d,e], Peter Szucs[d,e], Boris V. Safronov[a,b,*]

Abstract

Referred pain is a phenomenon of feeling pain at a site other than the site of the painful stimulus origin. It arises from a pathological mixing of nociceptive processing pathways for visceral and somatic inputs. Despite numerous studies based on unit recordings from spinal and supraspinal neurons, the exact mechanism and site of this mixing within the central nervous system are not known. Here, we selectively recorded from lamina I neurons, using a visually guided patch-clamp technique, in thoracic spinal cord preparation with preserved intercostal (somatic) and splanchnic (visceral) nerves. We show that somatic and visceral C fibers converge monosynaptically onto a group of lamina I neurons, which includes both projection and local circuit neurons. Other groups of lamina I neurons received inputs from either somatic or visceral afferents. We have also identified a population of lamina I local circuit neurons showing overall inhibitory responses upon stimulation of both nerves. Thus, the present data allow us to draw two major conclusions. First, lamina I of the spinal cord is the first site in the central nervous system where somatic and visceral pathways directly converge onto individual projection and local circuit neurons. Second, the mechanism of somatovisceral convergence is complex and based on functional integration of monosynaptic and polysynaptic excitatory as well as inhibitory inputs in specific groups of neurons. This complex pattern of convergence provides a substrate for alterations in the balance between visceral and somatic inputs causing referred pain.

Keywords: Convergence, Integration, Referred pain, Imaging, Dorsal horn, Action potential

1. Introduction

Referred pain is a phenomenon of feeling pain at a site other than the site of the painful stimulus origin. It arises in the viscera and is felt or "referred" in somatic tissues. Referred pain has been described for a number of organs, and it is generally believed that its origin depends on the way neuronal circuits, which process somatic and visceral information, are organized. Although several theories of somatovisceral integration at peripheral, spinal, and supraspinal levels have been proposed to explain this phenomenon, the precise neural substrate of referred pain is unknown.[10,13,33,41,42,47,49,53]

One of the most widely accepted theories of referred pain suggests that somatic and visceral inputs converge within the spinal cord.[41,47] In agreement with this, unit responses of dorsal horn neurons to stimulation of both visceral and somatic afferents have been reported in a number of in vivo studies.[1,2,4,6,9,16,32] However, little is known about the detailed organization of the neuronal network underlying somatovisceral integration in the superficial dorsal horn or whether both types of afferents directly contact any specific class of neurons.

Spinal lamina I is a key element in the nociceptive processing system. It receives inputs from thin afferents innervating the skin, joints, muscles, and viscera,[7,8,12] which project through ascending tracts to specific areas of the brain stem and thalamus.[25] Our group has shown that Aδ and C fibers from several dorsal roots can synapse directly on lamina I neurons, suggesting their possible role as integrators of a broad range of multimodal sensory inputs.[36] However, the spinal cord preparation we used in that study did not allow us to distinguish between somatic and visceral afferent inputs.

Here, we have made visually controlled whole-cell recordings from lamina I neurons, in an in vitro thoracic spinal cord preparation with preserved intercostal and splanchnic nerves, to show that somatic and visceral nociceptive C fibers converge monosynaptically onto a group of lamina I neurons. These neurons included both anterolateral tract projection neurons and local circuit neurons. Other groups of lamina I neurons received inputs from either somatic or visceral afferents, but not both. These findings suggest that different groups of lamina I neurons form the neuronal network processing somatic, visceral, and converging somatovisceral sensations.

2. Methods

2.1. Preparation of thoracic spinal cord with attached intercostal and splanchnic nerves

Wistar rats (P10-P14) were killed in accordance with the national guidelines (Direcção Geral de Veterinária, Ministério da Agricul-tura) under deep Na^{+}-pentobarbital anesthesia (30 mg/kg,

intraperitoneally) as determined by the lack of pedal withdrawal reflexes. The vertebral column with the dorsal part of the rib cage attached (between segments T4 and L1) was quickly cut out and immersed in oxygenated artificial cerebrospinal fluid (see 2.2. Recording) at room temperature. After removing the parietal pleura and dorsal peritoneal layer, the right greater splanchnic nerve was exposed along the vertebral bodies. The nerve was cut just proximal to the celiac ganglion and cleaned for subsequent stimulation with a suction electrode. The intercostal T9 nerve was also exposed between the ribs for stimulation with a suction electrode. The preparation was then turned over to allow dorsal laminectomy on vertebrae T4-T10. The dura mater was opened in the region of interest with fine forceps and scissors to provide access for recording pipettes. The preparation was glued (dorsal side up) with cyanoacrylate adhesive to a gold plate and transferred into a recording chamber (**Fig. 1A**).

2.2. Recording

Lamina I neurons were visualized in spinal segments T8 and T9 using the oblique infrared LED imaging technique (**Fig. 1A**).[44,52] Whole-cell recordings were made from visualized neurons using an EPC-10 amplifier (HEKA, Lambrecht, Germany),[30,31,52] while the preparation was bathed in artificial cerebrospinal fluid containing (in millimolars) NaCl 115, KCl 3, $CaCl_2$ 2, $MgCl_2$ 1, glucose 11, NaH_2PO_4 1, and $NaHCO_3$ 25 (pH 7.4 when bubbled with 95%–5% mixture of O_2–CO_2). Pipettes were pulled from thick-walled glass (BioMedical Instruments, Zöllnitz, Germany) and fire polished (resistance, 4-5 MΩ). The internal pipette solution contained (in millimolars) KCl 3, K-gluconate 150, $MgCl_2$ 1, BAPTA 1 and

HEPES 10 (pH 7.3 adjusted with KOH, final $[K^+]$ was 161 mM), and 1% biocytin. Signals were low-pass filtered at 2.9 kHz and sampled at 10 kHz. Offset potentials were compensated before seal formation. Liquid junction potentials were calculated and corrected for using the compensation circuitry in the amplifier. The AMPA glutamate receptor blocker CNQX was obtained from Sigma. All measurements were made at 22°C to 24°C.

Input resistance was measured in current-clamp mode from the response evoked by injection of a hyperpolarizing current pulse (10-20 pA, 500 ms duration). Resting membrane potential was measured with a balanced amplifier input.[46] In all current-clamp experiments, neurons were maintained either at their resting potentials or at a potential of −70 mV. Five types of intrinsic firing pattern were classified according to descriptions given for superficial dorsal horn neurons.[17,24,28,31,38,43] Tonic neurons were able to support regular action potential (AP) discharge during the depolarization evoked by current pulse injections (500 ms long). Adapting neurons fired several spikes that were confined to the beginning of depolarization. Burst neurons generated one or several bursts of 2 to 4 spikes each during tonic firing; the first burst appeared at the onset of depolarization. Delayed firing neurons exhibited a considerable time delay before the first APs appeared. Rhythmic neurons constantly/spontaneously discharged APs at zero current injection[24,28]; resting membrane potential could therefore not be determined for neurons from this group.

2.3. Stimulation of somatic and visceral nerves

The intercostal T9 and greater splanchnic peripheral nerves were stimulated using suction electrodes as described in Pinto
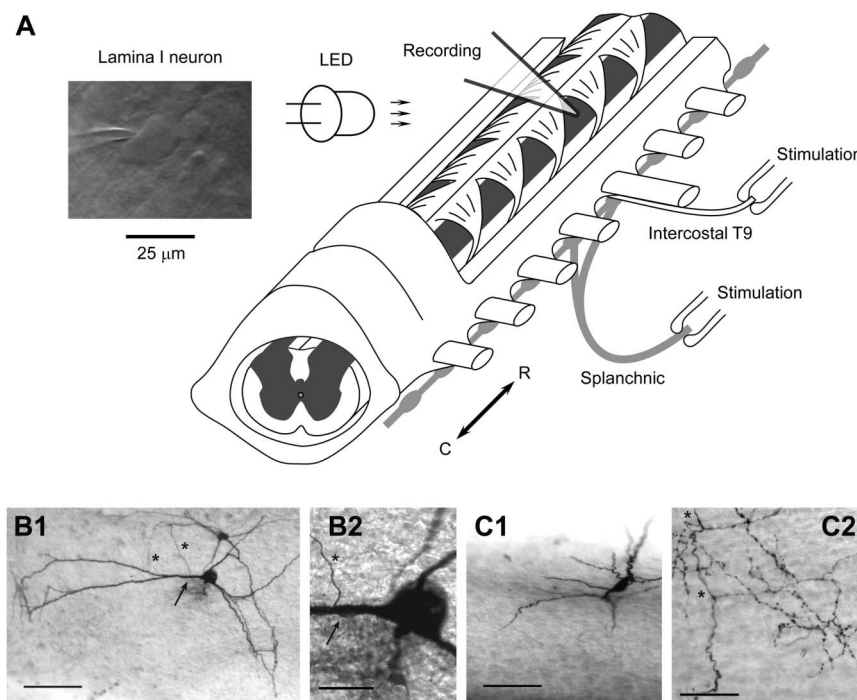

Figure 1. Spinal cord preparation to study somatovisceral convergence. (A) Preparation of the thoracic spinal cord with attached intercostal T9 and splanchnic nerves. The nerves were stimulated using suction electrodes. A lamina I neuron was viewed using oblique infrared LED illumination. (B1) Low magnification photograph of a projection neuron. This is a flattened neuron with extensive dendrites, one of which gives rise to a single axon (arrow). The axon descends towards deeper laminae after a short loop (asterisks) without further branching. Scale bar, 100 μm. (B2) High magnification photograph of the initiation point (arrow) of the projection axon (asterisk). Scale bar, 25 μm. (C1) Low magnification photograph of a local circuit neuron, with a fusiform somatodendritic morphology. The soma is located on the surface, while the dendrites (out of focus) protrude ventrally into lamina II. Scale bar, 100 μm. (C2) High magnification photomicrograph of the typical local circuit neuron axon. The main axon (asterisk) is thicker with regular swellings, while frequent side branches are thin and possess numerous varicosities, some of which have a diameter >1.5 μm. Scale bar, 50 μm. Recordings from the neurons shown in (B1) and (B2) and (C1) and (C2) are given in Figs. 5A and B, respectively.

et al.[35,36] using an isolated pulse stimulator (2100; A-M Systems, Carlsborg, WA). Each suction electrode had its own reference electrode, and the stimulation intensities used did not evoke any cross-stimulation of nerves.[35] A 50 μs wide pulse of increasing amplitude (0-150 μA, 10 μA increments, 1 Hz) was applied to recruit all Aδ fibers and a 1 ms pulse (0-150 μA, 10 μA increments, 0.1 Hz) to activate both Aδ and C fibers. Traces shown in all figures were recorded after saturating stimulations that recruited all inputs (1 ms, 100 μA; unless otherwise stated). Monosynaptic excitatory postsynaptic currents (EPSCs) were identified on the basis of low failure rates and short latency variations as previously described.[27,35,36]

The fiber conduction velocity (CV) was calculated from the measured length of the stimulated afferent nerve and conduction time. For the intercostal T9 nerve, the pathway was measured, before each experiment, from the distal cut end to the spinal cord midline and ranged between 9 and 15 mm. For the splanchnic nerve, the length of the pathway was measured in 3 groups of control animals and included the distance from the cut end (proximal to the celiac ganglion) to the sympathetic chain plus the path from the sympathetic chain to the middle of the T9 segment plus the mediolateral distance from the sympathetic chain to the spinal cord midline. These pathways were 11.5 ± 0.9 mm (n = 8) in P10 and P11, 12.4 ± 1.1 mm (n = 5) in P12, and 13.4 ± 0.7 mm (n = 8) in P13 and P14 animals. For both nerves, the length of the nerve within the suction electrode was measured from digital

photographs (range, 0.6-1.8 mm) and subtracted from the lengths given above. The conduction time was calculated for a monosynaptic EPSC with an allowance of 1 ms delay for synaptic transmission. The latencies were measured from the end of a 50 μs pulse for Aδ fibers and from the middle point of the 1 ms pulse for C fibers.

Afferent CVs were determined by recording compound AP currents[34] at 22°C to 24°C in the intercostal T9 nerve and the splanchnic nerve with the fragment of the sympathetic chain isolated from the spinal cord. For the intercostal nerve, the slowest Aδ afferents had CVs of 1.05 ± 0.12 m/s (n = 6; range, 0.84-1.63 m/s), whereas CV for the fastest C fibers was 0.56 ± 0.02 m/s (n = 6; range, 0.50-0.66 m/s). In the splanchnic nerve, the fastest C fibers had CVs of 0.55 ± 0.14 m/s (n = 5; range, 0.26-0.94 m/s). The Aδ component was observed only in 1 of 5 cases, probably, because the myelinated fibers account for less than 6% of the total number of fibers in the greater splanchnic nerve in adult rat[22] and because we used young animals. As lamina I neurons did not show inputs from visceral Aδ afferents, their CV was not analyzed further.

Based on these measurements, monosynaptic EPSCs recorded in lamina I neurons were classified as Aδ-fiber-mediated if they were evoked by 50 μs (100 μA) stimulations and the afferent CV was higher than 0.9 m/s. If the CV was below 0.6 m/s, the monosynaptic EPSC was considered as C-fiber-mediated. In some cases, EPSCs were mediated through fast

Table 1

Properties of inputs to lamina I neurons from intercostal and splanchnic nerves.

		Input from the intercostal nerve (n = number of neurons)		
		Suprathreshold	**Subthreshold/No**	**Inhibitory**
Input from the splanchnic nerve (n = number of neurons)	Suprathreshold	Total, n = 16; PN,* n = 3; LCN,† n = 3; rhythmic, n = 1	Total, n = 6; PN,‡ n = 1	Total, n = 3; LCN,§ n = 2; rhythmic, n = 1
		Mono In.Sp., n = 14 (PN, n = 3; LCN, n = 3)	Mono In.Sp., n = 1	Mono In.Sp., n = 2 (LCN, n = 1)
		Mono In., n = 2	Mono Sp., n = 5 (PN, n = 1)	Mono Sp., n = 1 (LCN)
		Somatovisceral	*Visceral*	*Visceral*
	Subthreshold/No	Total, n = 3; PN,‖ n = 2	Total, n = 15; PN,¶ n = 1; LCN,# n = 2; rhythmic, n = 2	Total, n = 6; LCN,** n = 2; rhythmic, n = 4
		Mono In.Sp., n = 1	Mono In.Sp., n = 1	
		Mono In., n = 2 (PN, n = 2)	Mono In., n = 5 (LCN, n = 1)	Mono In., n = 4 (LCN, n = 2)
			Mono Sp., n = 4	Mono Sp., n = 1
		Somatic		
	Inhibitory		Total, n = 3; PN,†† n = 1; rhythmic, n = 2	Total, n = 6; PN,‡‡ n = 1; LCN,§§ n = 4; rhythmic, n = 5
				Mono In.Sp., n = 1 (LCN)
			Mono In., n = 1	Mono In., n = 1
				Inhibition

This table provides data for 58 neurons that received inputs from one or both nerves. Neurons were classified on the basis of the overall effect of nerve stimulations. Input was considered as inhibitory if the overall effect of nerve stimulation was hyperpolarizing; some responses classified as inhibitory had monosynaptic excitatory components. Neurons were identified as projecting or local circuit based on axon trajectory.
Neurons classified according to morphology[26] and intrinsic firing patterns include the following:
* Flattened tonic, flattened tonic, and flattened burst.
† Multipolar tonic, flattened adapting, and fusiform tonic.
‡ Flattened burst.
§ Multipolar tonic and flattened tonic.
‖ Flattened tonic and flattened tonic.
¶ Flattened tonic.
# Multipolar tonic and flattened rhythmic.
** Multipolar rhythmic and multipolar rhythmic.
†† Flattened rhythmic.
‡‡ Flattened tonic.
§§ Flattened rhythmic, fusiform rhythmic, fusiform rhythmic, and multipolar rhythmic.
LCN, identified local circuit neuron; mono In., monosynaptic input identified for intercostal nerve only; mono In.Sp., monosynaptic components identified for both intercostal and splanchnic nerves; mono Sp., monosynaptic input from splanchnic nerve only; PN, anatomically identified anterolateral tract projection neuron; rhythmic, number of rhythmically firing neurons in a group.

afferents (CV > 0.9 m/s); these required 1 ms (100 µA) stimulation and were classified as high-threshold Aδ fibers. Fibers with CVs between 0.6 and 0.9 m/s were considered to be of the C type if a 1 ms stimulation was required to evoke an EPSC. Afferent inputs were classified as suprathreshold if at least 6 of 10 consecutive stimulations of the nerve (duration, 1 ms) evoked firing in lamina I neurons. Inputs classified in this study as subthreshold, with one exception (4 spikes), only evoked firing in 1 to 3 stimulations or showed excitatory postsynaptic potentials (EPSPs) that did not evoke spikes. All data are given as mean ± SEM unless otherwise stated.

2.4. Histological processing and cell identification

After fixation of the whole preparation in 4% paraformaldehyde and 2% glutaraldehyde, the spinal cord was carefully removed from the vertebral column and embedded in agar, and para-sagittal serial sections of 100 µm thickness were prepared with a tissue slicer (VT1000 S; Leica, Wetzlar, Germany). To visualize biocytin-filled neurons, the sections were permeabilized with 50% ethanol and treated according to the avidin-biotinylated horseradish peroxidase method (ExtrAvidin-Peroxidase, diluted 1:1000) followed by a diaminobenzidine chromogen reaction. Sections were counterstained with 1% toluidine blue and mounted in DPX (Fluka, Buchs, Switzerland). Photomicrographs were taken with a Primo Star microscope (Zeiss, Jena, Germany) equipped with a Guppy digital camera (Allied Vision

Technologies, Stadtroda, Germany). Contrast and brightness of the images used for the figures were adjusted using Adobe Image Ready software. Lamina I neurons were identified as either projection neurons or local circuit neurons by post hoc analysis of their axon structure and pathway in the spinal cord. The axon of a projection neuron entered the contralateral anterolateral tract, whereas that of local circuit neurons branched extensively within the ipsilateral dorsal horn with no branch ever crossing the spinal cord midline.

3. Results

The following experiments were designed to study the organization, efficacy, and monosynaptic or polysynaptic nature of somatic and visceral afferent inputs to individual lamina I neurons. We also tested whether both types of afferents directly converged onto identified projection and local circuit neurons. Sixty-six thoracic lamina I neurons were tested for inputs from both nerves. Fifty-eight responded to stimulation of at least one of the nerves and form the data set in our study. Successful labeling with biocytin was achieved for 22 neurons, which were anatomically identified as projection (n = 9; **Figs. 1B1, B2**) or local circuit neurons (n = 13; **Figs. 1C1, C2**). For labeled neurons, the cell body areas measured in parasagittal sections were 465.1 ± 139.9 µm^2 (mean ± SD; n = 9) for projection neurons and 433.7 ± 142.4 µm^2 (mean ± SD; n = 13; range, 218-707 µm^2) for local circuit neurons. Thus, these local circuit neurons belonged to a group of large lamina I interneurons.[3]
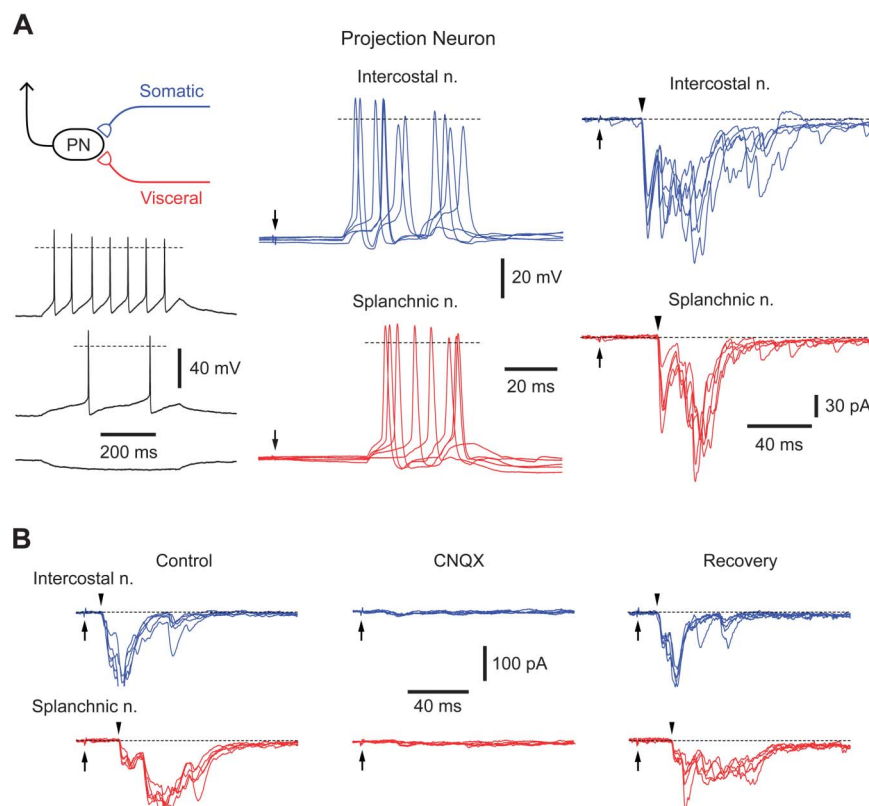

Figure 2. Somatovisceral lamina I neurons. (A) Recording from a lamina I projection neuron receiving suprathreshold inputs from the intercostal (blue traces) and splanchnic nerves (red traces). Left, Intrinsic firing pattern of this projection neuron; injected currents were (from top to bottom) +20, +10, and −10 pA. Dashed line in current-clamp indicates 0 mV. Middle, Current-clamp recording of excitatory postsynaptic potentials and spikes activated by stimulating intercostal and splanchnic nerves (pulse, 1 ms, 100 µA). Each panel shows 5 consecutive traces. Arrows indicate the time of nerve stimulation. Right, Voltage-clamp recordings of excitatory postsynaptic currents (EPSCs) evoked by stimulation of intercostal and splanchnic nerves (holding potential, −70 mV). Each panel shows EPSCs from 5 consecutive stimulations. Arrowheads indicate monosynaptic components. (B) Suppression of evoked EPSCs in an unidentified lamina I neuron by 10 µM CNQX. The nerves were stimulated by a 150 µA pulse (1 ms duration).
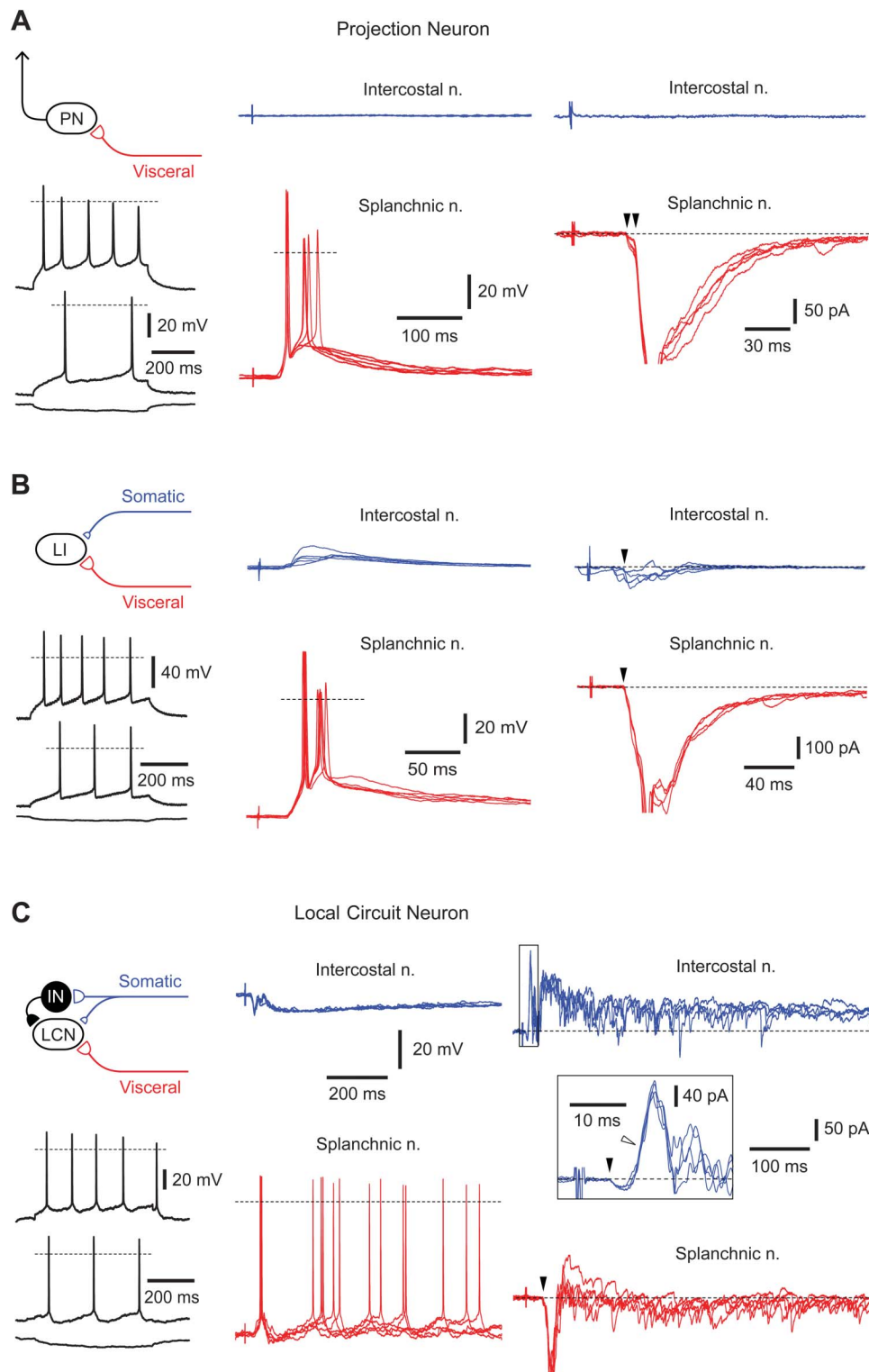
Figure 3. Neurons with dominating visceral inputs. (A) A lamina I projection neuron with suprathreshold visceral C-afferent input. The monosynaptic excitatory postsynaptic currents (EPSCs) are indicated by arrowheads (voltage-clamp, −70 mV). For monosynaptic inputs, 5 consecutive traces are superimposed. Intrinsic firing properties are shown for the injected currents of +70, +40, and −20 pA. (B) A nonidentified lamina I neuron with suprathreshold visceral and subthreshold somatic inputs. Monosynaptic EPSCs (indicated by arrowheads) were mediated by somatic and visceral C afferents (holding potential, −70 mV). Five consecutive traces are superimposed for current- and voltage-clamp. Intrinsic firing properties, injected currents are +100, +50, and −20 pA. C, A local circuit neuron with suprathreshold visceral and inhibitory somatic inputs. Note that although intercostal nerve stimulation evoked monosynaptic Aδ- (filled arrowhead) and C-fiber (not indicated) EPSCs (voltage-clamp, −70 mV), the overall response was inhibitory (current-clamp). The short-latency inhibitory postsynaptic current was disynaptic (open arrowhead, voltage-clamp) and Aδ-fiber-mediated. The splanchnic nerve stimulation activated a time-locked first spike (triggered by the monosynaptic C-fiber excitatory postsynaptic potential) followed by a repetitive discharge caused by polysynaptic excitatory postsynaptic potentials. For intrinsic firing properties, injected currents were +30, +20, and −20 pA. Schematic drawing shows possible organization of synaptic inputs to this local circuit neuron.

The mean input resistance of the neurons studied was 0.8 ± 0.1 GΩ (n = 51), and the resting potential was -74.2 ± 1.5 mV (n = 36). The summary of all inputs together with the anatomical types and intrinsic firing properties of identified neurons is given in **Table 1**.

3.1. Neurons with suprathreshold input from both somatic and visceral afferents

The largest group of neurons (16 of 58; 28%) received suprathreshold inputs from both intercostal and splanchnic nerves (**Fig. 2A** and **Table 1**). Good labeling was achieved for 6 of these neurons: 3 were projection neurons and 3 local circuit neurons; the body area of local circuit neurons was 364.5 ± 39.3 μm^2 (n = 3). In this group, 14 neurons received monosynaptic inputs from intercostal and splanchnic nerves (11 neurons received input from somatic and visceral C fibers, 2 neurons received input from somatic high-threshold Aδ fibers and visceral C fibers, and 1 neuron received input from somatic high-threshold Aδ and C fibers and visceral C fibers). The remaining 2 neurons received monosynaptic somatic (1 from C fibers and 1 from high-threshold Aδ and C fibers) as well as suprathreshold polysynaptic visceral inputs. The monosynaptic and polysynaptic EPSCs evoked by stimulating both nerves were suppressed by the AMPA glutamate receptor blocker CNQX (10 μM, **Fig. 2B**, n = 6).

3.2. Neurons with suprathreshold input from visceral afferents

Suprathreshold visceral input was recorded in 9 neurons, of which 1 was anatomically identified as a projection neuron and 2 as local circuit neurons. All neurons from this group received monosynaptic C-fiber-driven components. These neurons could be subdivided further according to their somatic inputs (**Fig. 3** and **Table 1**). In 3 neurons (including 1 projection neuron), there was no input from the intercostal nerve (**Fig. 3A**). As other neurons recorded in the same preparations showed inputs from the intercostal nerve, the lack of response is unlikely to be caused by nerve damage. In another 3 cases, stimulation of the intercostal nerve evoked only subthreshold polysynaptic or monosynaptic C-fiber-driven responses (**Fig. 3B**). In the remaining 3 neurons (including 2 local circuit neurons), the overall effect of intercostal nerve stimulation was inhibitory (**Fig. 3C**). Although all these cells received polysynaptic excitatory inputs and 2 of them additionally received monosynaptic inputs from Aδ and C fibers (1 neuron) or C fibers (1 neuron), somatic nerve stimulation caused pronounced

hyperpolarization (**Fig. 3C**). The inhibition had a disynaptic component[28] and was driven by both Aδ and C afferents (**Fig. 3C**).

3.3. Neurons with suprathreshold input from somatic afferents

Three neurons received suprathreshold inputs from the intercostal nerve but showed no or only a weak response to splanchnic nerve stimulation (**Fig. 4** and **Table 1**). Two of them were identified as projection neurons. All neurons in this group received direct C-fiber inputs from the intercostal nerve, whereas only one of them exhibited a weak monosynaptic input from the splanchnic nerve.

3.4. Subthreshold somatic and visceral responses

The second large population of neurons tested (15 of 58; 26%) received subthreshold inputs from both intercostal and splanchnic nerves (not shown; described in **Table 1**). This group included 1 identified projection neuron and 2 local circuit neurons. Monosynaptic inputs from both nerves were observed in 1 neuron, whereas 9 received direct C-fiber inputs from either the intercostal nerve (n = 5) or splanchnic nerve (n = 4). The remaining 5 neurons received only polysynaptic EPSPs/EPSCs.

3.5. Somatic and visceral inhibition

Stimulation of both nerves elicited overall inhibitory responses in 6 neurons. One of them was identified as a projection neuron with a tonic pattern of intrinsic firing (**Fig. 5A**), and the inhibition in this neuron was mediated through C afferents from both nerves.

It is interesting to note that the remaining 5 cells in this group were all rhythmically firing neurons, 4 of which could be identified as local circuit neurons (**Table 1**) with a cell body area of 490.0 ± 101.0 μm^2 (n = 4). One of these local circuit neurons is shown in **Figures 5B1-B5**. Stimulation of either nerve evoked C-fiber-driven EPSPs (monosynaptic and polysynaptic) and triggered one or several extra spikes, which were followed by a prolonged inhibition and interruption of rhythmic discharge (**Figs. 5B2-B3**).

4. Discussion

We have shown that somatic and visceral thin-fiber afferents converge directly onto a group of lamina I neurons, which includes both projection and local circuit neurons. Synaptic input
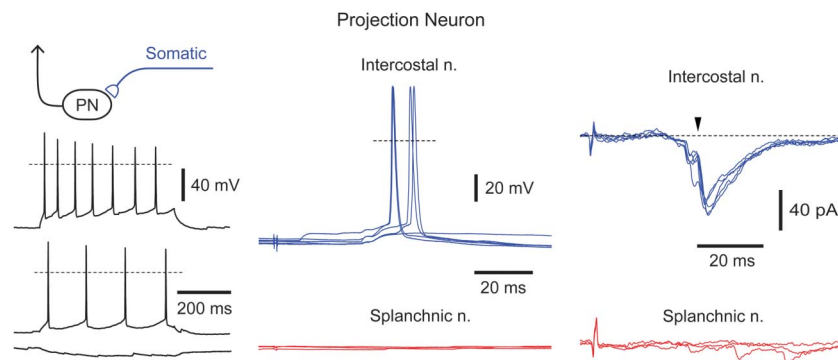

Figure 4. Neurons with dominating somatic inputs. Recordings from a projection neuron receiving suprathreshold somatic but no visceral input. Somatic excitatory postsynaptic potentials and excitatory postsynaptic currents are C-fiber-mediated. The monosynaptic excitatory postsynaptic current is indicated by an arrowhead. For the intercostal nerve, 5 consecutive traces are shown superimposed in current and voltage-clamp (holding potential, -70 mV). Intrinsic firing properties are shown for the injected currents of $+80$, $+30$, and -10 pA.
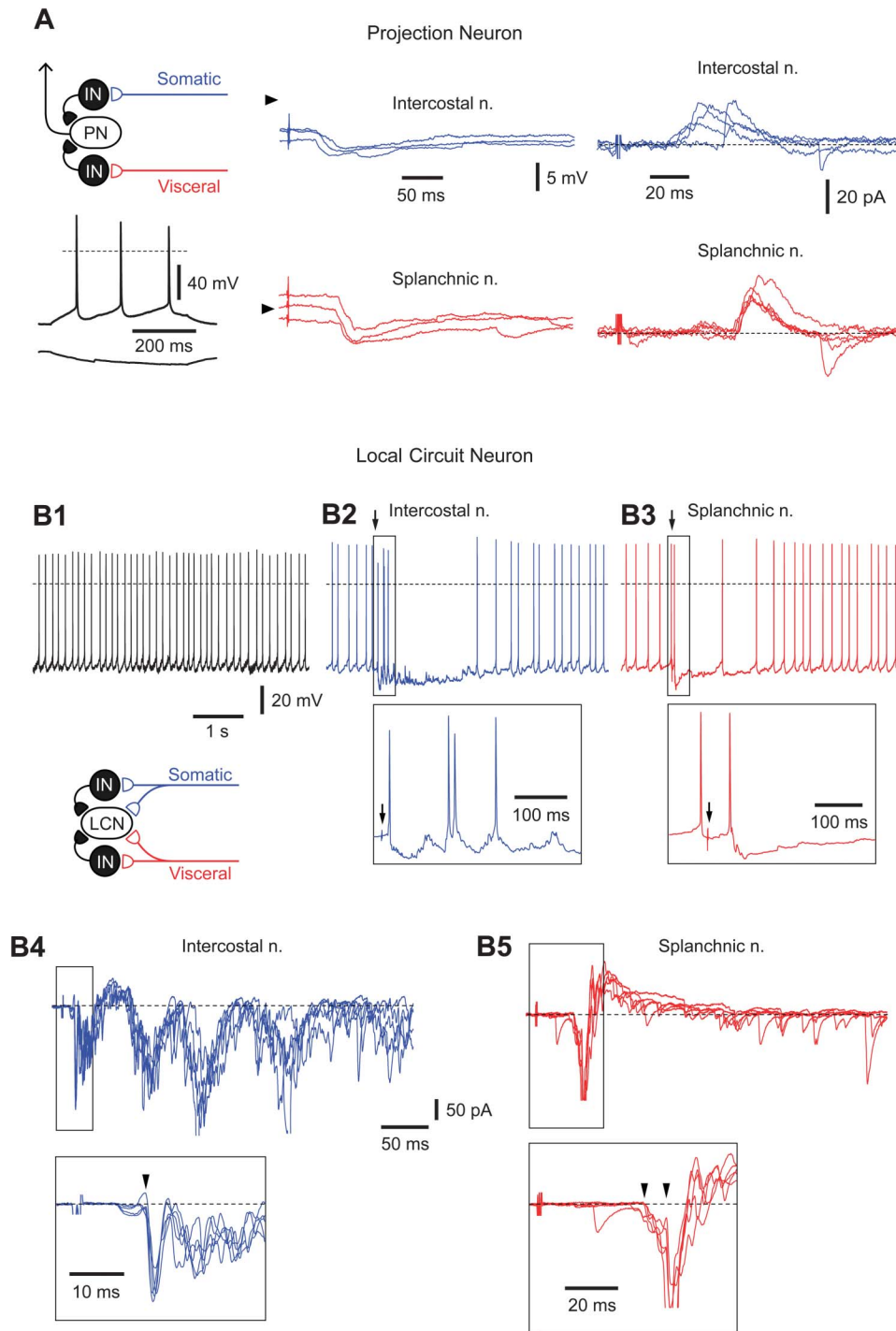
Figure 5. Neurons with inhibitory inputs. (A) Current- and voltage-clamp recordings of responses evoked in a projection neuron after stimulation of intercostal and splanchnic nerves. The neuron showed a tonic pattern of intrinsic firing (injected currents, +20 and −10 pA). Arrowheads in current-clamp indicate a potential of −70 mV. In voltage-clamp, the holding potential was −70 mV. (B1-B5) Recordings from a rhythmically firing local circuit neuron receiving a complex pattern of synaptic inputs from both nerves. Current-clamp, Recording of rhythmic firing in control (B1) and after stimulation (indicated by an arrow) of intercostal (B2) and splanchnic (B3) nerves. Note, the stimulation evoked one or several extra spikes (shown in the insets) followed by a prolonged inhibition of the discharge. Voltage-clamp, Recordings of excitatory postsynaptic currents and inhibitory postsynaptic currents activated by stimulating intercostal (B4) and splanchnic (B5) nerves. Monosynaptic excitatory postsynaptic currents are indicated by arrowheads in the insets. Schematic drawing illustrates possible organization of synaptic inputs to this local circuit neuron.

from both afferents was suprathreshold and evoked reliable discharge in some projection neurons. Therefore, lamina I can be considered as the first site in the central nervous system where somatic and visceral processing pathways converge onto the same neuron. Monosynaptic convergence of C-fiber afferents on projection neurons represents the most direct, reliable, and simple mechanism for central somatovisceral integration (**Fig. 6**). At the same time, our data show a complex organization of spinal sensory circuits, which include somatic- and visceral-specific as well as inhibitory pathways.
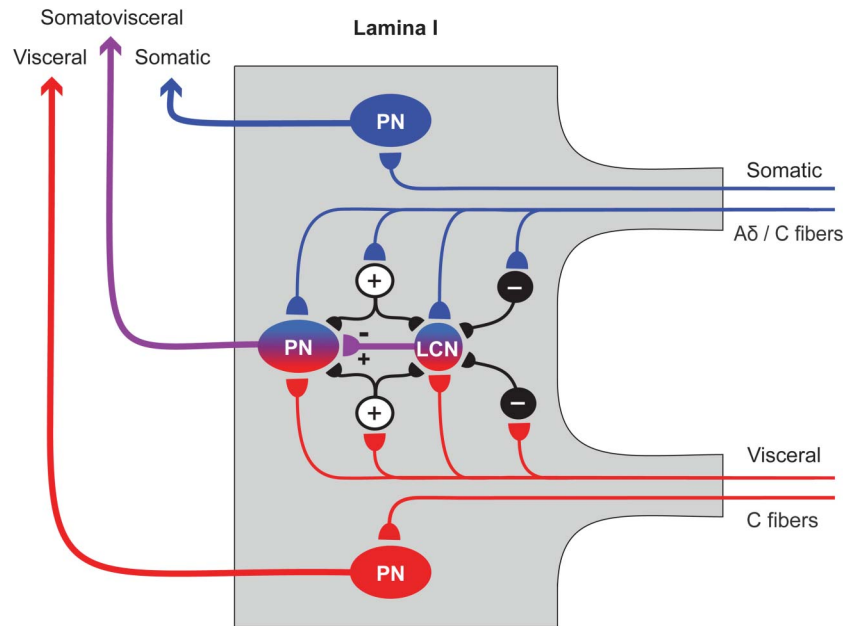
Figure 6. Proposed model of somatovisceral convergence of thin afferents onto lamina I neurons. Somatic (blue) and visceral (red) afferents converge directly onto a lamina I projection neuron (PN) and a lamina I local circuit neuron (LCN), where somatic and visceral processing pathways merge together. Lamina I LCNs can be both inhibitory[51] and excitatory[27] and can directly synapse on PNs.[27] Intercalated excitatory (+) and inhibitory (−) neurons are shown by smaller circuits; their laminar location is not known. The excitatory intercalated neurons may amplify the primary afferent-driven input to a PN. The inhibitory intercalated neurons may play diverse roles, eg, disinhibit a PN by supressing activity in a rhythmic inhibitory LCN, or induce reciprocal inhibition of somatic or visceral inputs. At the same time, other PNs receive somatic- or visceral-specific inputs.

As an experimental model, we have chosen the thoracic spinal cord preparation with attached greater splanchnic and intercostal T9 nerves. The visceral afferents in the greater splanchnic nerve supply the stomach, small intestine, proximal colon, spleen, pancreas, and mesenteric vessels.[15] The somatic afferents within the intercostal nerve supply segmental areas of the skin, ribs, costal cartilages, and intercostal muscles.[20] Thin afferents from visceral and somatic sensory receptors terminate in the superficial dorsal horn[7,8] and, as shown by unit recordings, can converge onto dorsal horn neurons.[4,6,9,29,32] This study further shows that one-quarter of the recorded lamina I neurons process mixed somatic and visceral information and that both projection and local circuit neurons receive monosynaptic converging C-fiber inputs. In addition, suprathreshold responses usually contained a strong polysynaptic excitatory component. Therefore, our data indicate that neuronal network of lamina I plays an important role in amplifying primary afferent signals (**Fig. 6**).[18,23,45,54]

We have also found neurons that were excited by stimulating either somatic or visceral afferents, suggesting the existence of modality-specific pathways. These data, however, should be considered with some caution because we may have underestimated the total somatic input. A single intercostal nerve or dorsal root projects rostrocaudally to several spinal cord segments,[7,11,50] and as a consequence of this anatomical arrangement, a single superficial dorsal horn neuron responds to stimulation of several roots.[35,36] Therefore, assertions regarding inputs to these neurons measured after stimulation of one intercostal nerve are likely to underestimate somatic input. This may also explain why a smaller number of neurons were excited by somatic vs visceral afferents in our study.

Neurons from the group receiving subthreshold inputs from both nerves may play a critical role in alteration of somatovisceral integration and induction of referred pain. They can undergo

modality-specific sensitization and change their processing mode after induction of functional plasticity, eg, at synapses of primary afferents[21] or excitatory interneurons mediating polysynaptic responses.[45] Such plasticity could alter the balance between somatic and visceral information as it flows to supraspinal processing centers. However, it is also possible that the neurons studied in our in vitro preparation may have lower excitability than those in vivo experimental models.

Previous research in rats showed that electrical stimulation of intercostal afferents inhibits the firing of thoracic spinal neurons elicited by noxious stimulation of visceral afferent nerves.[39] This phenomenon can be explained by our observation that some lamina I neurons receive suprathreshold or subthreshold excitatory visceral inputs together with inhibitory somatic inputs. This way, somatovisceral convergence may not only contribute to visceral referred pain but also be a mechanism for turning off visceral nociceptive pathways. Furthermore, inhibition of lamina I neurons mediated through somatic Aδ and C afferents described here can explain a classical observation that rather strong natural "counter-irritative" somatic stimuli are required to supress visceral pain, whereas brushing of the hairs of the corresponding region has little or no effect.[40,48]

The physiological roles of neurons with inhibitory inputs from both nerves may be diverse. The overall inhibitory inputs, in the majority of cases, were observed in local circuit neurons that exhibited the rhythmic pattern of intrinsic firing. Rhythmically firing lamina I neurons have recently been described in several reports.[5,24,28] Many of these neurons were identified as GABAergic local circuit neurons because their axons were immunoreactive for the vesicular GABA transporter and branched densely within laminae I and II.[51] Thus, afferent-driven inhibitory inputs to these cells may transiently disinhibit their postsynaptic targets in the superficial dorsal horn and thus increase the efficacy of excitatory inputs to projection neurons (**Fig. 6**). However, some

lamina I local circuit neurons were identified as excitatory interneurons directly supplying projection neurons.[27] In this case, the afferent-driven inhibition of the local circuit neuron may selectively reduce the efficacy of somatic or visceral pathways in excitation of nociceptive projection neurons. This mechanism of control of Aδ- and C-fiber inputs to lamina I neurons may resemble classical reciprocal inhibition studied by unit recordings of somatic and visceral Aβ and Aδ afferent inputs to deep spinal neurons in cat[19,37,48] and monkey.[14]

Finally, referred pain is well documented for several organs (eg, heart, lung, liver, kidney, colon, and uterus). This implies that its neural substrate involves neuronal circuitries that process both somatic and visceral sensations. This study reveals that the functional coupling between the thin afferents onto lamina I neurons is the first step in central somatovisceral integration and may be considered as a neurophysiological basis of referred pain. The emergence of referred pain may arise in the lamina I network because of changes in the efficacy of somatovisceral, somatic, and visceral inputs.

Conflict of interest statement

The authors have no conflicts of interest to declare.

Acknowledgements

References

[1] Akeyson EW, Schramm LP. Processing of splanchnic and somatic input in thoracic spinal cord of the rat. Am J Physiol 1994;266:R257–267.

[2] Akeyson EW, Schramm LP. Splanchnic and somatic afferent convergence on cervical spinal neurons of the rat. Am J Physiol 1994;266:R268–276.

[3] Al Ghamdi KS, Polgar E, Todd AJ. Soma size distinguishes projection neurons from neurokinin 1 receptor-expressing interneurons in lamina I of the rat lumbar spinal dorsal horn. Neuroscience 2009;164:1794–804.

[4] Alarcon G, Cervero F. The effects of electrical stimulation of A and C visceral afferent fibres on the excitability of viscerosomatic neurones in the thoracic spinal cord of the cat. Brain Res 1990;509:24–30.

[5] Baccei ML. Pacemaker neurons and the development of nociception. Neuroscientist 2014;20:197–202.

[6] Cervero F. Somatic and visceral inputs to the thoracic spinal cord of the cat: effects of noxious stimulation of the biliary system. J Physiol 1983;337:51–67.

[7] Cervero F, Connell LA. Distribution of somatic and visceral primary afferent fibres within the thoracic spinal cord of the cat. J Comp Neurol 1984;230:88–98.

[8] Cervero F, Connell LA. Fine afferent fibers from viscera do not terminate in the substantia gelatinosa of the thoracic spinal cord. Brain Res 1984;294:370–4.

[9] Cervero F, Lumb BM. Bilateral inputs and supraspinal control of viscerosomatic neurones in the lower thoracic spinal cord of the cat. J Physiol 1988;403:221–37.

[10] Craig AD. Pain mechanisms: labeled lines versus convergence in central processing. Annu Rev Neurosci 2003;26:1–30.

[11] Cruz F, Lima D, Coimbra A. Several morphological types of terminal arborizations of primary afferents in laminae I-II of the rat spinal cord, as shown after HRP labeling and Golgi impregnation. J Comp Neurol 1987;261:221–36.

[12] Dostrovsky JO, Craig AD. Ascending projection systems. In: McMahon SB, Koltzenburg M, editors. Wall and Melzack's textbook of pain. Philadelphia: Elsevier Churchill Livingstone, 2006. p. 187–203.

[13] Farrell K, Keely S, Graham B, Callister R. A systematic review of the evidence for central nervous system plasticity in animal models of inflammatory-mediated gastrointestinal pain. Inflamm Bowel Dis 2014;20:176–95.

[14] Foreman RD, Hancock MB, Willis WD. Responses of spinothalamic tract cells in the thoracic spinal cord of the monkey to cutaneous and visceral inputs. PAIN 1981;11:149–62.

[15] Furness JB. Peripheral autonomic nervous system. In: Paxinos G, editor. The rat nervous system: Academic Press, San Diego, CA. 2014. p. 61–76.

[16] Gokin AP, Kostyuk PG, Preobrazhensky NN. Neuronal mechanisms of interactions of high-threshold visceral and somatic afferent influences in spinal cord and medulla. J Physiol (Paris) 1977;73:319–33.

[17] Graham BA, Brichta AM, Callister RJ. In vivo responses of mouse superficial dorsal horn neurones to both current injection and peripheral cutaneous stimulation. J Physiol 2004;561:749–63.

[18] Graham BA, Brichta AM, Callister RJ. Moving from an averaged to specific view of spinal cord pain processing circuits. J Neurophysiol 2007;98:1057–63.

[19] Hancock MB, Rigamonti DD, Bryan RN. Convergence in the lumbar spinal cord of pathways activated by splanchnic nerve and hind limb cutaneous nerve stimulation. Exp Neurol 1973;38:337–48.

[20] Hebel R, Stromberg MW. Anatomy and embryology of the laboratory rat. Wörthersee: BioMed Verlag, 1986.

[21] Ikeda H, Heinke B, Ruscheweyh R, Sandkuhler J. Synaptic plasticity in spinal lamina I projection neurons that mediate hyperalgesia. Science 2003;299:1237–40.

[22] Isomura G, Iwata S, Chiba M, Shimizu N. Constitution of the greater splanchnic nerve in the rat. Anat Anz 1985;159:159–71.

[23] Kato G, Kawasaki Y, Koga K, Uta D, Kosugi M, Yasaka T, Yoshimura M, Ji RR, Strassman AM. Organization of intralaminar and translaminar neuronal connectivity in the superficial spinal dorsal horn. J Neurosci 2009;29:5088–99.

[24] Li J, Baccei ML. Pacemaker neurons within newborn spinal pain circuits. J Neurosci 2011;31:9010–22.

[25] Lima D, Almeida A. The medullary dorsal reticular nucleus as a pronociceptive centre of the pain control system. Prog Neurobiol 2002;66:81–108.

[26] Lima D, Coimbra A. A Golgi study of the neuronal population of the marginal zone (lamina I) of the rat spinal cord. J Comp Neurol 1986;244:53–71.

[27] Luz LL, Szucs P, Pinho R, Safronov BV. Monosynaptic excitatory inputs to spinal lamina I anterolateral-tract-projecting neurons from neighbouring lamina I neurons. J Physiol 2010;588:4489–505.

[28] Luz LL, Szucs P, Safronov BV. Peripherally driven low-threshold inhibitory inputs to lamina I local-circuit and projection neurones: a new circuit for gating pain responses. J Physiol 2014;592:1519–34.

[29] Ma WL, Zhang WB, Xiong KH, Guo F. Visceral and orofacial somatic afferent fiber terminals converge onto the same neuron in paratrigeminal nucleus: an electron microscopic study in rats. Auton Neurosci 2007;131:45–9.

[30] Melnick IV, Santos SF, Safronov BV. Mechanism of spike frequency adaptation in substantia gelatinosa neurones of rat. J Physiol 2004;559:383–95.

[31] Melnick IV, Santos SF, Szokol K, Szucs P, Safronov BV. Ionic basis of tonic firing in spinal substantia gelatinosa neurons of rat. J Neurophysiol 2004;91:646–55.

[32] Milne RJ, Foreman RD, Giesler GJ Jr, Willis WD. Convergence of cutaneous and pelvic visceral nociceptive inputs onto primate spinothalamic neurons. PAIN 1981;11:163–83.

[33] Pierau FK, Fellmer G, Taylor DC. Somato-visceral convergence in cat dorsal root ganglion neurones demonstrated by double-labelling with fluorescent tracers. Brain Res 1984;321:63–70.

[34] Pinto V, Derkach VA, Safronov BV. Role of TTX-sensitive and TTX-resistant sodium channels in Adelta- and C-fiber conduction and synaptic transmission. J Neurophysiol 2008;99:617–28.

[35] Pinto V, Szucs P, Derkach VA, Safronov BV. Monosynaptic convergence of C- and Adelta-afferent fibres from different segmental dorsal roots on to

single substantia gelatinosa neurones in the rat spinal cord. J Physiol 2008;586:4165–77.

[36] Pinto V, Szucs P, Lima D, Safronov BV. Multisegmental A{delta}- and C-fiber input to neurons in lamina I and the lateral spinal nucleus. J Neurosci 2010;30:2384–95.

[37] Pomeranz B, Wall PD, Weber WV. Cord cells responding to fine myelinated afferents from viscera, muscle and skin. J Physiol 1968;199:511–32.

[38] Prescott SA, De Koninck Y. Four cell types with distinctive membrane properties and morphologies in lamina I of the spinal dorsal horn of the adult rat. J Physiol 2002;539:817–36.

[39] Qin C, Farber JP, Linderoth B, Shahid A, Foreman RD. Neuromodulation of thoracic intraspinal visceroreceptive transmission by electrical stimulation of spinal dorsal column and somatic afferents in rats. J Pain 2008;9:71–8.

[40] Ruch TC. Pathophysiology of pain. In: Ruch TC, Patton HD, Woodbury JW, Towe AL, editors. Neurophysiology. Philadelphia: Saunders, 1961. p. 350–68.

[41] Ruch TC. Visceral sensation and referred pain. In: Fulton JF, editor. Howell's textbook of physiology. Philadelphia: Saunders, 1947. p. 385–401.

[42] Rucker HK, Holloway JA. Viscerosomatic convergence onto spinothalamic tract neurons in the cat. Brain Res 1982;243:155–7.

[43] Ruscheweyh R, Ikeda H, Heinke B, Sandkuhler J. Distinctive membrane and discharge properties of rat spinal lamina I projection neurones in vitro. J Physiol 2004;555:527–43.

[44] Safronov BV, Pinto V, Derkach VA. High-resolution single-cell imaging for functional studies in the whole brain and spinal cord and thick tissue blocks using light-emitting diode illumination. J Neurosci Methods 2007;164:292–8.

[45] Santos SF, Luz LL, Szucs P, Lima D, Derkach VA, Safronov BV. Transmission efficacy and plasticity in glutamatergic synapses formed by excitatory interneurons of the substantia gelatinosa in the rat spinal cord. PLoS One 2009;4:e8047.

[46] Santos SF, Melnick IV, Safronov BV. Selective postsynaptic inhibition of tonic-firing neurons in substantia gelatinosa by mu-opioid agonist. Anesthesiology 2004;101:1177–83.

[47] Selzer M, Spencer WA. Convergence of visceral and cutaneous afferent pathways in the lumbar spinal cord. Brain Res 1969;14:331–48.

[48] Selzer M, Spencer WA. Interactions between visceral and cutaneous afferents in the spinal cord: reciprocal primary afferent fiber depolarization. Brain Res 1969;14:349–66.

[49] Sinclair DC, Weddell G, Feindel WH. Referred pain and associated phenomena. Brain 1948;71:184–211.

[50] Szentagothai J. Neuronal and synaptic arrangement in the substantia gelatinosa rolandi. J Comp Neurol 1964;122:219–239.

[51] Szucs P, Luz LL, Pinho R, Aguiar P, Antal Z, Tiong SY, Todd AJ, Safronov BV. Axon diversity of lamina I local-circuit neurons in the lumbar spinal cord. J Comp Neurol 2013;521:2719–41.

[52] Szucs P, Pinto V, Safronov BV. Advanced technique of infrared LED imaging of unstained cells and intracellular structures in isolated spinal cord, brainstem, ganglia and cerebellum. J Neurosci Methods 2009;177:369–80.

[53] Theobald G. Referred pain: a new hypothesis. Colombo: Times of Ceylon, 1941.

[54] Todd AJ. Neuronal circuitry for pain processing in the dorsal horn. Nat Rev Neurosci 2010;11:823–36.